MODEL-BASED ESTIMATION OF SURFACE GEOMETRY USING PASSIVE POLARIMETRIC IMAGING

Charles D. Creusere, Ketan Mehta, and David G. Voelz
Klipsch School of Electrical and Computer Engineering
New Mexico State University

1. INTRODUCTION

The polarization signature of the light that reflects from an object contains information about that object's material composition as well as its shape, its roughness, and its surface features. Thus, it makes sense to exploit this information in practical image processing applications like scene segmentation and object recognition. For remote image sensing in the visible optical band, a passive system (i.e., the illumination source is the Sun) is generally required, but capturing consistent polarimetric signatures using such a system is challenging because the signature depend upon both the target's material properties and the relative source/target/camera geometry. In previous work, we have shown how multiple views of the target object from different positions can be used to create a consistent estimate of its index of refraction by fitting a generating model to the acquired data [1]. Unlike previous work that focused on exploiting passive polarization in imaging systems (e.g., [2, 3, 4, 5, 6, 7, 8]), the model-based approach that we developed in [1] provides us with a classification feature vector (the index of refraction) that is highly robust to the relative scene geometry [9]. In this paper, we are interested in extracting another parameter from the polarimetric signature which is equally robust by fitting the same underlying pBRDF model of the generating process that we used in our previous work. This time, however, we are interested in estimating the mean surface normal angle of each facet of the object being imaged. As an example, knowing these surface normal angles would allow one to determine planes of the roof of a building being imaged from above (even if they were all made of the same material) which could facilitate identification of that building.

2. POLARIMETRIC BIDIRECTIONAL REFLECTANCE DISTRIBUTION FUNCTION (PBRDF) MODEL

Our approach for extracting estimates of the local planar structure of the target requires that polarimetric images be captured from multiple known positions relative to the target location. This can be easily accomplished from an aerial platform moving towards a target object by logging GPS locations and time stamps during each capture and correlating these to the ground position using mapping software. It is assumed that each of the captured polarimetric images is generated by the same underlying model—in this case, the microfacet pBRDF model for specular reflection proposed by Priest and Meier [10]—and that by solving for the parameters which best fit this

This research was supported by the National Geospatial-Intelligence Agency through contract HM1582-0601-2036

model, one can make progressively better estimates for each image pixel. Figure 1 shows the geometry assumed for the estimation process and the associated polarimetric BRDF is given by

$$d\mathbf{L}_{\mathrm{r}}(\theta_r, \varphi_r) = \mathbf{F}(\theta_i, \varphi_r, \varphi_r - \varphi_i) d\mathbf{E}(\theta_i, \varphi_i) \quad (1)$$

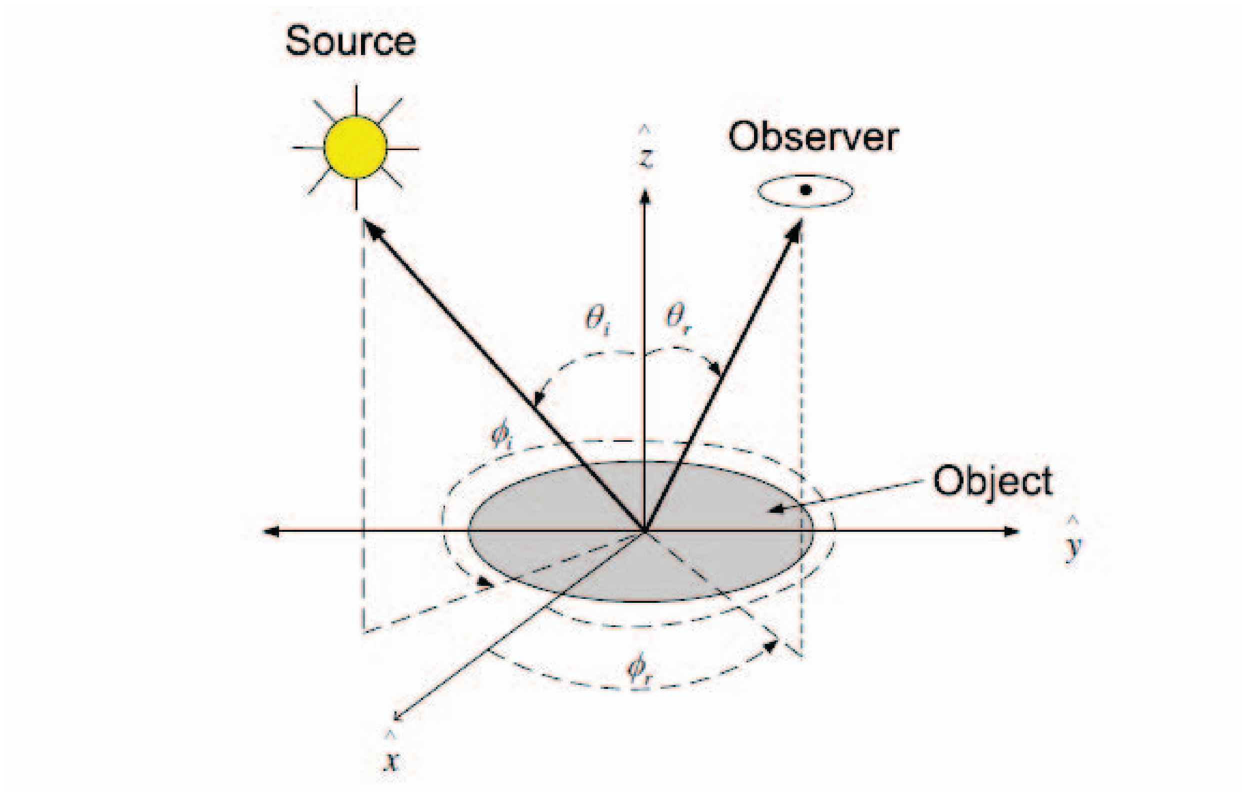

Fig. 1. Bidirectional reflectance distribution function (BRDF) Geometry

where **F** is the pBRDF Mueller matrix, $\mathbf{L_r}$ is the reflected Stokes vector and **E** is the incident Stokes vector. A Stokes vector is a four element vector that completely characterizes the polarization of an optical field. The interested reader is referred to standard optics textbooks [11, 12] for a detailed treatment of Stokes vectors and Mueller matrices. The Priest and Meier pBRDF model used here assumes that a rough surface is composed of a collection of microfacets, each of which obeys Fresnel's equations [11] and that all polarization effects in the reflected image are caused by single surface reflection. The expression for the pBRDF Mueller matrix is given by

$$f_{jl}(\theta i, \theta r, \varphi i - \varphi r) = \frac{exp(-tan^2(\theta)/2\sigma^2))}{2\pi \times 4\sigma^2 \times cos^4(\theta) \times cos(\theta i) cos(\theta r)} \times m_{jl}(\theta i, \theta r, \varphi i - \varphi r) \quad (2)$$

where f_{jl} denotes the element in the j^{th} row and l^{th} column of the pBRDF Mueller matrix F, m_{jl} denotes the element in the j^{th} row and l^{th} column of the Fresnel reflectance Mueller matrix

M, θ is the angle of orientation of the microfacets relative to the object surface normal, φ is given by $\varphi = \varphi_i - \varphi_r$ and σ describes the surface roughness [10].

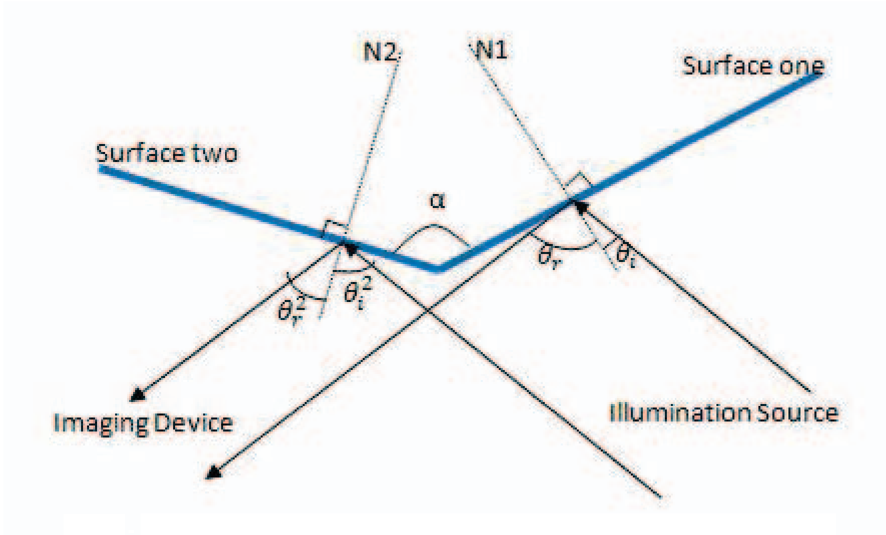

Fig. 2. Reflection for the case of a two surface object

It is the parameter θ that we are interested in estimating here. To form our estimate, we make measurements at multiple θ_r with θ_i being kept constant. We then find the parameters for (2) within the framework of (1) which best fit the observations. The resulting system of nonlinear equations is solved using the Levenberg-Marquardt (LM) optimization algorithm [13]. Unfortunately, the quality of the resulting solution depends heavily on the initialization of algorithm. We consider this aspect of the problem in the next section.

3. SUCCESSIVE REINITIALIZATION

To overcome the problems associated with initialization, we apply a process of successive reinitialization. Specifically, we divide the Stokes images (pixels of which correspond to single elements of the Stokes vector captured at a given spatial location) into non-overlapping regions and apply LM optimization within the region using different random initializations. We then evaluate the solutions resulting from each of these different initializations to determine a consensus decision—i.e., the most common solution in the region to within some tolerance. An estimate for the model parameter is thus calculated for each of the regions individually. The final estimate is an average of all these individual estimates. The process is repeated and the optimizations are rerun over all the regions, by using this mean estimate as the initial optimization condition. If the solutions for most of the regions are now consistent, we accept it as the correct solution and output the model parameters. If not, we declare that block as being of mixed type containing more than one surface orientation, in this case). We note that dynamically adapting the block size would almost certainly improve the overall performance as well as make the algorithm more flexible.

4. RESULTS

We have initially validated our approach using computer-based simulations of in-plane two surface scattering as shown in Figure 2 with our ultimate goal here being to determine the angle α between the two surfaces. The position of the illumination source was varied from 45° to 85° in 5° increments with the reflection angle fixed at 65°, and Gaussian noise of varying power is added to simulate measurement errors and volumetric scattering. Table 1 summarizes our results where 100 Monte Carlo trials have been performed (each an application of the full optimization algorithm) with the index of refraction of the target object being assumed to be known (this is not a major limitation since we have previously shown that it can be estimated with sufficient accuracy [1]). Studying the table, we note that the worst-case error is 1.8 which occurs when the surfaces are closest to perpendicular as one would expect. The minimum error of 0.16 is achieved when the surfaces are almost parallel.

Table 3. Estimated value of angle α

True value of α	Estimated value of α	Absolute error	Percentage error
95	93.246	1.754	1.846
100	98.724	1.277	1.277
110	109.242	0.758	0.690
120	118.838	1.161	0.968
130	128.406	1.594	1.226
140	139.229	0.771	0.551
160	158.546	1.454	0.909
150	148.547	1.453	0.969
170	169.190	0.810	0.477
175	174.713	0.287	0.164

5. REFERENCES

[1] V. Thilak, D. G. Voelz, and C. D. Creusere, “Polarization-based index of refraction and reflection angle estimation for remote sensing applications,” *Appl. Opt.*, vol. 46(30), pp. 7527–7536, October 2007.

[2] L. B. Wolff, “A polarization-based material classification from specular reflection,” *IEEE Trans. Pattern Anal. Machine Intell.*, vol. 12, pp. 1059–1071, November 1990.

[3] H. Chen and L. B.Wolff, “Polarization phase-based method for maaterial classification and object recognition in computer vision,” in *Proc. IEEE Computer Society Conference on Computer Vision and Pattern Recognition*, June 1996, pp. 128– 135.

[4] H. Chen and L. B. Wolff, “Polarization phase-based method for material classification in computer vision,” *International Journal of Computer Vision*, vol. 28(1), pp. 73–83, June 1998.

[5] D. M. McKeown, S. D. Cochran, S. J. Ford, J. C. McGlone, J. A. Shufelt, and D. A. Yocum, “Fusion of hydice hyperspectral data with panchromatic imagery for catographic feature extraction,” vol. 37, pp. 1261–1277, March 1999.

[6] D. Slater and G. Healey, “Material classification for 3d objects in aerial hyperspectral images,” in *Proc. IEEE Computer Society Conference on Computer Vision and Pattern Recognition*, June 1999, p. 2268.

[7] S. Tominaga and S. Okamoto, “Reflectance-based material classification for printed circuit boards,” in *Proc.* 12th *Conference on Image Analysis and Processing*, 2003, pp. 238–244.

[8] J. Zallat, P. Grabbling, and Y. V. Takakura, “Using polarimetric imaging for material classification,” in *Proc. IEEE International Conference on Image Processing*, Barcelona, Spain, Sept. 2003, pp. 827–830.

[9] V. Thilak, C. D. Creusere, and D. G. Voelz, “Material classification from passive polarimetric imagery,” in *Proc. IEEE Int’l Conf. Image Proc.*, Sept. 2007, vol. IV, pp. 121–124.

[10] R. G. Priest and S. R. Meier, “Polarimetric microfacet scattering theory with applications to absorptive and reflective surfaces,” *Opt. Eng.*, vol. 41(5), pp. 988–993, May 2002.

[11] E. Hecht, *Optics*, Addison-Wesley, Reading, MA, 2005.

[12] M. Bass, *Handbook of Optics vol. 1*, McGraw Hill, New York, 1995.

[13] P.E. Gill and W. Murray, “Algorithms for the solution of the nonlinear least-sqaures problem,” *SIAM J. Numer. Anal.*, vol. 15, pp. 977–992, October 1978.